# Prion Protein Peptides Induce α-Helix to β-Sheet Conformational Transitions†

Jack Nguyen,‡ Michael A. Baldwin,‡ Fred E. Cohen,§,|| and Stanley B. Prusiner*,‡,||

*Departments of Neurology, Medicine, Pharmaceutical Chemistry, and Biochemistry and Biophysics, University of California, San Francisco, California 94143-0518*

*Received October 26, 1994; Revised Manuscript Received January 11, 1995*⊗

ABSTRACT: The structures of synthetic peptides corresponding to regions of putative secondary structure in the cellular prion protein $PrP^C$ were studied as models for the conformational transition that features in the formation of the pathogenic isoform, $PrP^{Sc}$. Transgenetic studies argue that these PrP isoforms interact during the formation of $PrP^{Sc}$, which involves the unfolding of one or more helices of $PrP^C$ followed by refolding into β-sheets. PrP residues 109−122 (H1), which were predicted to be α-helical, form β-sheets in aqueous buffers, while the longer peptide 104−122 (104H1) and also peptide 129−141 (H2) have coil or α-helical structures in solution. Both 104H1 and H2 were converted into β-sheets upon interaction with H1, as monitored by Fourier transform infrared (FTIR) and circular dichroism (CD) spectroscopy. The conversion was sequence-specific since mouse (Mo) H1, which differs from Syrian hamster (SHa) at two residues, was inefficient at converting SHa104H1 into the β-sheet form. In buffers containing 10% acetonitrile, 104H1 was converted into the β-sheet form by addition of as little as 1% H1. In addition, Aβ 11−25 and Aβ25−35 peptides with similar physical properties to H1 were incapable of converting H2 into the β-sheet form. How well these studies approximate the structural transitions in PrP that underlie the replication of prions remains to be established.

The prion protein (PrP)[1] is a glycosylphosphatidylinositol (GPI)-anchored sialoglycoprotein that plays a central role in the development of neurodegenerative diseases that can be sporadic, inherited, or infectious (Prusiner, 1991). Prion diseases of humans include kuru, Gerstmann−Sträussler−Scheinker syndrome (GSS), Creutzfeldt−Jakob disease (CJD), fatal familial insomnia (FFI), and diseases transmitted surgically from inadequately sterilized instruments or infected graft tissues, or by treatment with contaminated preparations of growth hormone. Animal prion diseases include scrapie of sheep and bovine spongiform encephalopathy (BSE or "mad cow disease") of cattle, which has reached epidemic proportions in the United Kingdom. The function of the normal, cellular protein ($PrP^C$) is unknown. Mice in which the PrP gene is ablated appear to develop normally (Büeler et al., 1992) but are resistant to infection with prions (Büeler et al., 1993; Prusiner et al., 1993a).

In prion diseases, $PrP^C$ is converted by a posttranslational process into an abnormal isoform, designated $PrP^{Sc}$ (Borchelt et al., 1990, 1992; Caughey & Raymond, 1991), which is the only known component of the infectious prion particle. Peptide mapping of $PrP^{Sc}$ with Edman sequencing and mass spectrometry revealed no differences between the amino acid sequence and that predicted from the PrP gene sequence (Stahl et al., 1993); furthermore, no chemical modifications were identified that might distinguish $PrP^{Sc}$ from $PrP^C$ (Stahl et al., 1992, 1993), although the conversion of $PrP^C$ to $PrP^{Sc}$ causes physical differences including enhanced protease resistance and decreased solubility. Despite the absence of a covalent distinction between $PrP^C$ and $PrP^{Sc}$, Fourier transform infrared (FTIR) spectroscopy and circular dichroism (CD) spectroscopy revealed a substantial conformational difference. $PrP^C$ is essentially α-helical with little or no β-sheet (Pan et al., 1993), whereas $PrP^{Sc}$ has a high β-sheet content and less α-helical structure (Pan et al., 1993; Safar et al., 1993b). N-Terminally truncated $PrP^{Sc}$, designated PrP 27−30, has even higher β-sheet content (Caughey et al., 1991; Gasset et al., 1993; Pan et al., 1993), consistent with its polymerization into amyloid (McKinley et al., 1991; Prusiner et al., 1983).

Secondary structure predictions based on the alignment of 11 mammalian and 1 avian PrP sequences (Gabriel et al., 1992; Harris et al., 1991) identified 4 putative helical regions, suggesting $PrP^C$ might be a 4-helix-bundle protein. Three-dimensional structural modeling was carried out using a heuristic approach to give a plausible tertiary structure model in which the hydrophobic helix−helix interactions would be disrupted by the known pathogenic mutations (Cohen et al., 1994; Huang et al., 1994). This revealed intriguing interactions including close proximity between residues 178 and 129; an Asp→Asn mutation at residue 178 causes different phenotypic diseases depending upon the presence of Val (linked to CJD) or Met (linked to FFI) at 129 (Goldfarb et al., 1992). However, in isolation three of four synthetic peptides (H1−H4) corresponding to the putative helical regions were found to adopt β-sheet structures in the solid state and in aqueous solution, from which amyloid fibrils precipitated (Gasset et al., 1992); only H2 showed any

† This work was supported by grants from the National Institutes of Health (NS14069, AG08967, AG02132, NS22786, and AG10770) and the American Health Assistance Foundation, as well as by gifts from the Sherman Fairchild and Bernard Osher Foundations.

* To whom correspondence should be addressed at the Department of Neurology, HSE-781, University of California, San Francisco, CA 94143-0518. Telephone: 415/476-4482. Fax: 415/476-8386.

‡ Department of Neurology.

§ Departments of Medicine and Pharmaceutical Chemistry.

|| Department of Biochemistry and Biophysics.

⊗ Abstract published in *Advance ACS Abstracts,* March 15, 1995.

[1] Abbreviations: PrP, prion protein; $PrP^C$, cellular isoform of PrP; $PrP^{Sc}$, scrapie isoform of PrP; GPI, glycosylphosphatidylinositol; FTIR, Fourier transform infrared; CD, circular dichroism; Hu, human; Mo, mouse; SHa, Syrian hamster; Tg, transgenic.

0006-2960/95/0434-4186$09.00/0 

Table 1: PrP and Aβ Peptides[a]

| name | residues | sequence |
|---|---|---|
| | PrP Peptides | |
| H1 | 109−122 | MKHMAGAAAAGAVV |
| H1(Mo) | 108−121 | LKHVAGAAAAGAVV |
| 104H1 | 104−122 | KPKTNMKHMAGAAAAGAVV |
| H2 | 129−141 | MLGSAMSRPMMHF |
| | Aβ Peptides | |
| Aβ(11−25) | 11−25 | EVHHQKLVFFAEDVG |
| Aβ(25−35) | 25−35 | GSNKGAIIGLM |

[a] Unless stated otherwise, the PrP peptides correspond to the Syrian hamster sequence.

significant tendency to adopt α-helical structure. Alternative predictions using other secondary structure algorithms were remarkably consistent as to which regions of the protein would possess ordered structure, but they disagreed as to whether α-helices or β-sheets would be favored (Huang et al., 1994), consistent with the observed conformational instability. Thus, these peptides may provide useful models for investigating the conformational transitions underlying conversion of $PrP^{C}$ into $PrP^{Sc}$.

A remarkable characteristic of prion diseases is that the conformational character of $PrP^{Sc}$ can be imposed on nascent $PrP^{C}$, thereby resulting in the "replication" of "infectious" prions. We report here that it may be possible to model some aspects of the conformational transition that PrP undergoes using synthetic PrP peptides. The conformational changes in PrP peptides are sequence-specific, which may reflect the profound influence of PrP sequences on the species barriers (Pattison, 1965) for transmission of prion diseases as demonstrated by studies with transgenic (Tg) mice expressing foreign PrP genes (Prusiner et al., 1990; Scott et al., 1993; Telling et al., 1994).

## EXPERIMENTAL PROCEDURES

The peptides employed in this study are identified in Table 1. The PrP peptides were synthesized from *N*-Fmoc-protected amino acids using either an Applied Biosystems (Foster City, CA) Model 430 automated synthesizer or a Millipore (Bedford, MA) Model 9050 Plus PepSynthesizer and purified by RP-HPLC. They were lyophilized, dissolved in dilute HCl, and lyophilized again to remove residual TFA. The purity was confirmed by electrospray mass spectrometry. Stock peptide solutions were made by weighing on a Cahn microbalance; the concentrations of selected solutions were confirmed by capillary electrophoresis with UV monitoring at 214 nm and amino acid analysis. $^{13}C$-Labeled Fmoc-amino acids were supplied by either Cambridge Isotope Laboratories (Woburn, MA) or Isotec (Miamisburg, OH). The incorporation and positions of the $^{13}C$ labels in the peptides were confirmed by mass spectrometry and tandem mass spectrometry.

Aβ(11−25) = EVHHQKLVFFAEDVG (Fraser et al., in press) was a generous gift from Dr. D. A. Kirschner, Harvard Medical School. It forms fibrils morphologically similar to H1 and its FTIR spectrum is characteristic of an antiparallel β-sheet. Aβ(25−35) = GSNKGAIIGLM, which also forms fibrils and is cytotoxic (Pike et al., 1993), was synthesized and purified as described above.

FTIR measurements were made by transmission spectroscopy using a Perkin Elmer (Norwalk, CT) System 2000 spectrometer equipped with a microscope attachment and purged with dry nitrogen. Solution spectra were recorded on 0.5 μL samples in $BaF_2$ cells with a path length of 0.05 mm. Peptide concentrations were 2.5−3.0 mM either in $D_2O$/20 mM Hepes (pD 7.2) (corrected)/100 mM NaCl (buffer A) or in mixtures of this with acetonitrile. Alternatively, thin films of dried peptide were analyzed by transmission. Typically, 100 FTIR spectra recorded at 2 $cm^{-1}$ resolution were averaged, converted from transmittance to absorbance, and smoothed, a buffer spectrum was subtracted, and they were normalized and plotted over the amide I frequency region (1700−1600 $cm^{-1}$) (Krimm & Bandekar, 1986). The ordinate scale in all spectra presented here is in arbitrary units.

For the data in Figure 2, FTIR spectra were monitored until the intensity of the low-frequency β-sheet (LF-β) signal at ~1623−1621 $cm^{-1}$ maximized (typically 48 h). They were deconvoluted, and a second derivative gave the frequencies of the absorption maxima, which were used for curve-fitting to the original data. The area of the LF-β absorption was determined as a percentage of the amide I band. These values were lower than the total β-sheet content as the high-frequency component was not taken into account, due to overlap with the β-turn absorption; the maximum LF-β content observed for any peptide was 80% for AGAAAAGA; H1 in 50% acetonitrile gave an LF-β content of 65%.

CD spectra were recorded on a Jasco Model 720 spectropolarimeter using 0.01 cm path length cylindrical quartz cells at room temperature. Peptide concentrations were 0.15−3.0 mM either in 20 mM Hepes (pH 7.2)/100 mM NaF (buffer B) or in mixtures of this with acetonitrile. The use of NaF avoided excessive light absorption by chloride ions below 200 nm. Typically, 20 spectra were recorded at a scan speed of 0.5 nm/s and accumulated. Qualitative secondary structure assignments were based on the following: α-helix, minima at 208 and 222 nm, maximum at 190 nm; β-sheet, minimum at 218 nm, maximum at 195 nm; random coil, minimum at 198 nm, no positive peak (Johnson, 1990).

Peptides for bioassays were maintained in stock solutions in hexafluoroisopropyl alcohol and were quantitated by amino acid analysis; 10 μM peptide solutions for inoculation were prepared by evaporating the solvent from measured aliquots and redissolving the peptides in inoculation buffer, which was phosphate-buffered saline (PBS). Alternatively, they were dispersed in 1,2-dioleoylphosphatidylglycerol sodium salt (DOPG), the solvent was evaporated, and PBS was added. Syrian hamsters (groups of eight) each received a 50 μL intracerebral inoculation of H1, H2, H3, and H4, or a combination of all four of the above, or of SHa 117−133. Tg mice expressing high levels of hamster $PrP^{C}$ (groups of 10) each received 30 μL of inoculum. All animals were monitored for symptoms of prion diseases for up to 2 years.

## RESULTS

The sequence MKHMAGAAAAGAVV (H1), corresponding to codons 109−122 of Syrian hamster (SHa) PrP, is the most N-terminal of the four predicted α-helical regions (Gasset et al., 1992). It was previously shown that this peptide is α-helical only in trifluoroethanol or hexafluoroisopropyl alcohol or when vacuum-dried as a thin film from one of these solvents. It rapidly converts to β-sheet in water

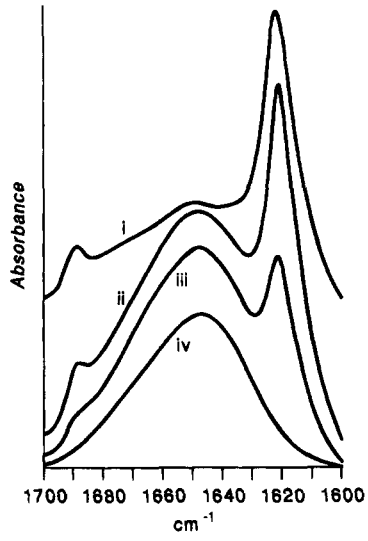


FIGURE 1: FTIR amide I spectra in $D_2O$/20 mM Hepes (pD 7.2)/100 mM NaCl (buffer A) showing the increase in α-helix/random coil signal (~1650 $cm^{-1}$) over β-sheet (1623 $cm^{-1}$) with the N-terminal lengthening of H1. (i) SHa PrP 109−122 (H1); (ii) 106−122; (iii) 105−122; and (iv) 104−122.

and precipitates as amyloid fibrils, a tendency that is even stronger in the shorter peptide AGAAAAGA (113−120). Other workers have reported similar observations for peptide 106−126 (Selvaggini et al., 1993), which was identified by monitoring the cytotoxicity of PrP peptides in neuronal cell cultures (Forloni et al., 1993), and peptide 118−133, which was predicted to form amyloid by a database search for the motif $(XGXX)_n$ (Come et al., 1993).

*N-Terminal Extension of H1 Induces a Conformational Change.* It seemed likely that the hydrophobic section of H1, which might be responsible for the amyloid-forming properties, could be offset by extending the N-terminus and thereby incorporate more hydrophilic residues; thus, longer peptides were synthesized that included lysines at 104 and 106. Extension of the N-terminus from residue 109 to 104 shifted the amide I peak maximum from 1623 to 1648 $cm^{-1}$ for FTIR spectra in aqueous buffer at physiological pH (Figure 1). Thus, 104−122 (104H1) was more stable in the α-helical or coil conformations than in the β-sheet conformation (Byler & Susi, 1986; Surewicz & Mantsch, 1988). FTIR does not always distinguish clearly between α-helices and coils: CD of 104H1 in aqueous buffers or as thin dry films gave spectra characteristic of coil, which changed to α-helix in 10% or more HFIP. This was reminiscent of many of the nascent helices characterized by 2D-NMR spectroscopy, which form α-helices under the influence of appropriate solvents only if an intrinsic helical propensity exists in the sequence (Dyson et al., 1988). Thus, peptide 104−122, KPKTNMKHMAGAAAAGAVV (104H1) provided a tool for monitoring conditions that might induce conformational changes to mirror those in PrP.

Acetonitrile is known to stabilize β-sheet structure (Taylor & Kaiser, 1987) and has been employed in studying the β-sheet conformations of the Alzheimer's Aβ peptides (Otvos et al., 1993). Acetonitrile is also a more efficient solvent for hydrophobic peptides such as H1. The effect of varying the acetonitrile content on the proportion of β-sheet for H1, 104H1, and 104H1 mixed with H1 as measured by FTIR is illustrated in Figure 2. Acetonitrile had little effect on H1 as the β-sheet form was stable in purely aqueous buffers. By contrast, 104H1 showed only a low level of β-sheet in aqueous buffers, and this was barely increased by 10% acetonitrile. However, the addition of 1 part H1 to 100 parts 104H1 in 10% acetonitrile converted a significant fraction of the 104H1 to β-sheet, and one part H1 in 10 parts 104H1 was sufficient to convert virtually all the 104H1 to β-sheet. With a 1:10 peptide ratio, further increasing the acetonitrile content to 50% had no additional effect. The proportion of the amide I band corresponding to the LF-β signal for 104H1 approached but never attained that of H1, probably because the additional residues within the extended peptide never adopted the β-sheet conformation. H1 was also able to induce the conversion of 104H1 to β-sheet in purely aqueous buffers, but only when the ratio of H1 to 104H1 approached 1:1.

*Species-Specific Amino Acid Differences Inhibit Peptide Interactions.* The rate of conversion from random coil or α-helices to β-sheets was monitored by CD. The spectra in Figure 3 compare the efficiency of the interactions between SHa 104H1 and H1 peptides corresponding to SHa and Mo sequences. The SHa/Mo sequences have two amino acid differences, Met/Leu at codon 109 and Met/Val at codon 112. DNA sequencing in apes and other nonhuman primates

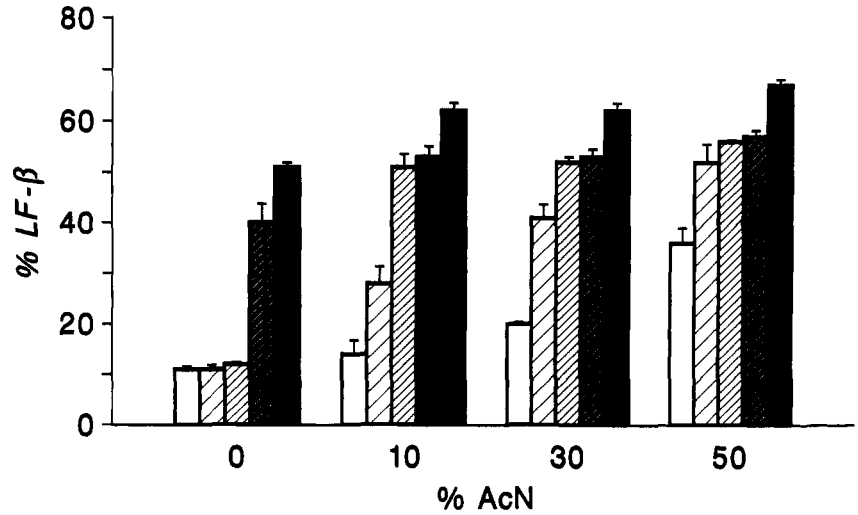


FIGURE 2: FTIR low-frequency β-sheet dependence on acetonitrile content of the buffer for mixtures of H1 and 104H1 (molar ratios). With bars at each % AcN from left to right: 104H1; 1:100 H1:104H1; 1:10 H1:104H1; 1:1 H1:104H1; H1.

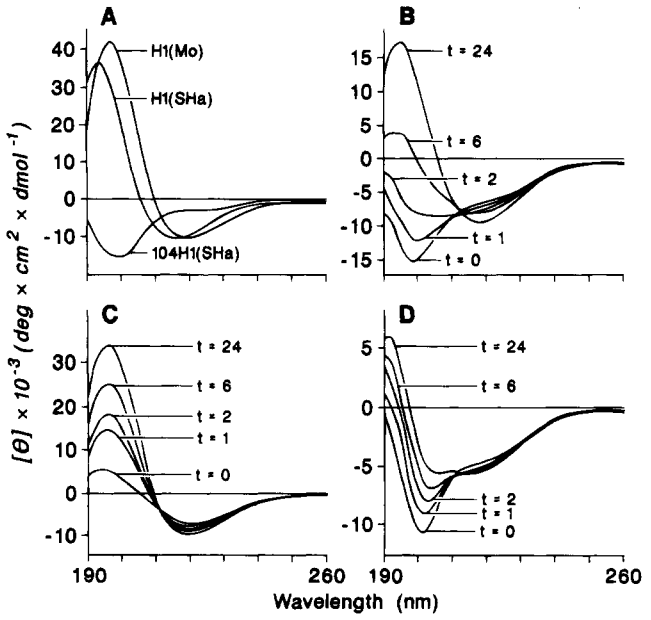


FIGURE 3: Changes in the CD spectra of 104H1 and H1 peptides corresponding to Syrian hamster (SHa) and mouse (Mo) sequences. Panel A: H1(Mo), H1(SHa), and 104H1(SHa) in buffer B/30% acetonitrile recorded after 24 h. Panel B: 104H1(SHa) mixed 10:1 with H1(SHa) recorded immediately after mixing and at intervals up to 24 h. Panel C: 104H1(SHa) mixed 1:1 with H1(SHa). Panel D: 104H1(SHa) mixed 1:1 with H1(Mo).

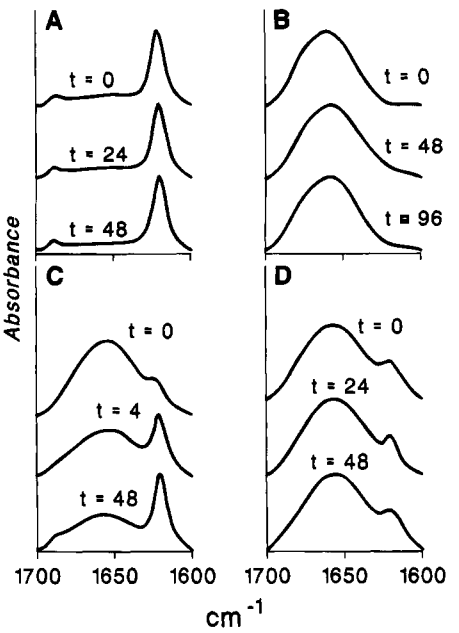


FIGURE 4: Changes in the FTIR amide I band with time of pure and mixed (1:1 molar ratio) peptides in 50% buffer A/50% acetonitrile: (A) H1; (B) H2; (C) H2/H1; and (D) H2/Aβ(11−25).

has demonstrated that this is a critical region in determining species barriers (Schätzl et al., 1995). The CD spectra in panel A of pure peptides in 30% acetonitrile show that the β-sheet was favored for both H1(SHa) and H1(Mo), whereas 104H1(SHa) was largely coil. Panels B and C show the homotypic interaction over time between the two SHa peptides mixed 10:1 (104H1:H1) and 1:1 in 30% acetonitrile, in both cases revealing a progressive conversion of coil to β-sheet that was virtually complete within 24 h. By contrast, heterotypic interaction of equimolar SHa 104H1 and Mo H1 illustrated in panel D yielded significantly less β-sheet, even after 24 h, as shown by the negative peak at 198−205 nm attributable to coil structures.

*H1/H2 Interactions Induce a Conformational Change.* Another target for conformational conversion is peptide H2 (SHa PrP residues 129−141), the only one of the four predicted helices that proved to be α-helical as a peptide (Gasset et al., 1992). Noncovalent interactions between peptides from different regions of a protein have been observed to enhance secondary structure when the same structure in the isolated peptides has only marginal stability (Wu et al., 1993). FTIR spectroscopy demonstrated that H1 formed β-sheets in 50% acetonitrile, in which it was soluble up to 5 mg/mL without fibril formation as monitored by electron microscopy, whereas H2 was α-helical or random coil (Figure 4, panels A and B). Neither of these observations changed with time whereas changes were observed in the FTIR amide I spectrum of a 1:1 mixture of H1/H2 in the same medium (panel C). The β-sheet conformation of H1 was initially inhibited by H2. The subsequent reduction in the signal at 1657 $cm^{-1}$ and the concomitant increase in the narrow peak at 1622 $cm^{-1}$ over a 48 h period indicated a progressive α→β conversion. Deconvolution of the 48 h spectrum revealed a higher β-sheet content than could be accounted for by H1 alone; therefore, a proportion of H2 was converted to β-sheet. The Alzheimer's disease-related peptides Aβ(11−25) and Aβ(25−35) both form amyloid structures, but neither was able to initiate the α→β conformational change in H2 [Panel D shows Aβ(11−25); data not shown for Aβ(25−35)]. Clearly, the induction in H2 of the α→β conformational transition was highly sequence-dependent.

*FTIR Spectroscopy of $^{13}C$-Labeled Peptides Confirms H1/104H1 and H1/H2 Interactions.* Dipole−dipole interactions in the antiparallel β-sheets of amyloid-forming proteins and peptides such as H1 split the FTIR amide I absorption into high- and low-frequency components, the latter being the most intense (Krimm & Bandekar, 1986). Thus the peak at 1650−1660 $cm^{-1}$ for coil or helices observed for 104H1 in aqueous ($D_2O$) medium (Figure 5, panel A, trace i) is split to give peaks at 1625 and 1690 $cm^{-1}$ for the antiparallel β-sheet of H1 under the same conditions (A, ii). The splitting is due to both inter- and intramolecular coupling. The β-sheet dipole−dipole interactions can be disrupted by the introduction of a single $^{13}C$ atom in place of a carbonyl $^{12}C$ in each molecule, raising the frequency of the $^{12}C$ carbonyl vibration from ~1625 to 1630−1640 $cm^{-1}$ (Halverson et al., 1991). The natural frequency of the $^{13}C$ amide vibration is somewhat lower, and intermolecular coupling between $^{13}C$ carbonyls in adjacent strands further reduces this to 1600−1610 $cm^{-1}$. This latter frequency shift provides a test for those residues of a peptide that are involved in intermolecular antiparallel β-sheet (Ashburn et al., 1992; Halverson et al., 1991).

Labeling H1 at the C-1 atom of Ala-116 revealed an amide I band with a new $^{13}C{=}O$ vibration at 1604 $cm^{-1}$ (A, iii). This frequency was affected significantly by mixing 1:1 with unlabeled H1, shifting it to 1611 $cm^{-1}$ (A, iv). The reduction in the splitting of the intermolecular signal demonstrated that the labeled and unlabeled molecules were intimately mixed within the β-sheet. Mixing labeled H1 with unlabeled 104H1 had a very similar effect, shifting the peak maximum to 1609 $cm^{-1}$ (A, v). Thus, we conclude not only that H1 converted the 104H1 into β-sheet but also that 104H1 was recruited into a common β-sheet with H1.

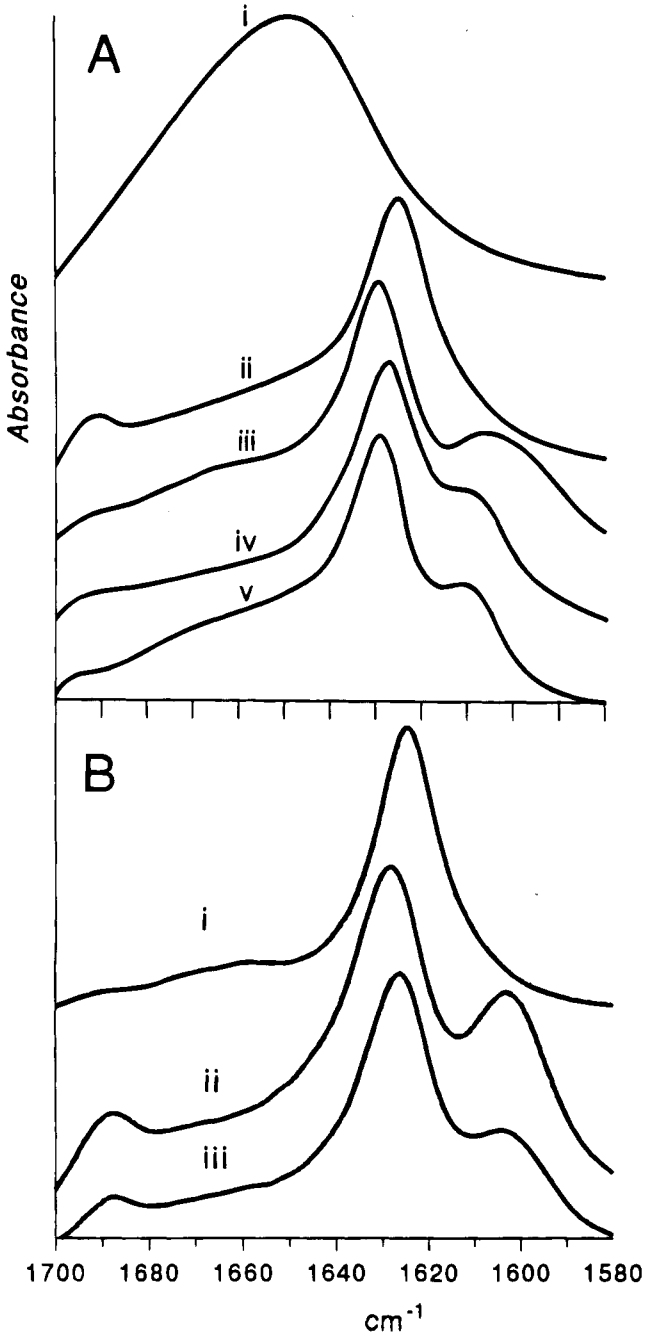


FIGURE 5: FTIR amide 1 spectra of $^{13}C$-labeled peptides [thin films deposited from solutions in 20 mM Hepes/100 mM NaCl/$D_2O$ (pD 7.2)]. (Panel A, trace i) Unlabeled 104H1; (A, ii) unlabeled H1; (A, iii) (Ala-116 $^{13}C{=}O$)H1; (A, iv) (Ala-116 $^{13}C{=}O$)H1 mixed 1:1 with unlabeled H1; (A, v) (Ala-116 $^{13}C{=}O$)H1 mixed 1:1 with unlabeled 104H1. (B, i) Unlabeled Mo H1; (B, ii) (Ala-117 $^{13}C{=}O$)-H1; (B, iii) (Ala-117 $^{13}C{=}O$)H1 mixed 1:1 with unlabeled Mo H1.

An alternative $^{13}C$-labeled peptide with the heavy isotope at C-1 of Ala-117 showed similar effects; it gave an FTIR spectrum (Figure 5, panel B, trace ii) very similar to that of the Ala-116-labeled peptide (A, iii). The FTIR spectrum of unlabeled Mo H1 (B, i) is similarly indistinguishable from that of unlabeled SHa H1 (A, ii). When isotopically labeled SHa H1 was mixed with unlabeled Mo H1, the low-frequency band decreased in intensity but it remained at 1604 $cm^{-1}$ and showed almost no frequency shift (B, iii). Thus, H1 peptides with two sequence differences do not interact but form two separate $\beta$-sheet structures. This provides another example of the sequence specificity of the interacting species that can be linked to the species barrier.

The amide 1 band of a 1:1 mixture of labeled H1 and unlabeled H2 in aqueous media ($D_2O$) revealed the presence of both helix or coil structures and $\beta$-sheet. In 30% acetonitrile, the IR spectrum changed to reflect the conversion of H2 to $\beta$-sheet under the influence of H1. The low-frequency peak due to $^{13}C{=}O$ moved from 1604 to 1607 $cm^{-1}$, showing incorporation of H2 into the $\beta$-sheets of H1, although the smaller degree of this shift was suggestive of a less ordered structure (data not shown).

*Peptide Oxidation Does Not Account for PrP Amyloid Formation.* It has been proposed that the aggregation and neurotoxicity of the A$\beta$ peptides are attributable to oxidation and free radical formation (Hensley et al., 1994). We monitored H1 and 104H1 stock solutions maintained in Eppendorf tubes at 4 °C over several weeks. The samples were opened periodically for aliquots to be removed but no attempt was made to exclude air. Capillary electrophoresis and electrospray mass spectrometry detected a small increase (~10%) in the abundance of full-length peptides containing methionine sulfoxide rather than methionine but no cleavage to shorter species. Oxidized H1 isolated and purified by HPLC showed lower $\beta$-sheet-forming tendencies than H1 itself. The H1-induced conformational transition of 104H1 to $\beta$-sheet gave identical results whether the samples were maintained in the presence of air or under nitrogen. Thus there is no evidence to suggest that oxidation features in these conformational transitions. H1 and 104H1 decomposed to smaller species when incubated with phosphate or HEPES buffers at 37 °C for 168 h, as described for A$\beta$ peptides (Hensley et al., 1994), but these conditions were unlike those employed in the present study.

*Peptides Fail To Exhibit Prion Infectivity.* Experiments were carried out to determine whether the peptides described here are capable of inducing prion diseases in animals. Syrian hamsters and Tg mice overexpressing SHa PrP were inoculated intracerebrally with 10 $\mu$M peptide solutions in PBS, both with and without the lipid DOPG, and monitored for symptoms characteristic of prion diseases. The peptides studied were H1, H2, H3, and H4, a combination of each of these, and SHa 118−133. No such symptoms developed during periods of up to 2 years. Whether the use of higher concentrations or longer peptides will induce prion infectivity remains to be established.

## DISCUSSION

While the importance of structural studies of the PrP isoforms in understanding the events that feature in prion replication are well appreciated, methodologic problems continue to plague such investigations. The low concentration of $PrP^C$ in brain, the inability to produce large amounts of $PrP^C$ by recombinant approaches, and the insolubility of both $PrP^{Sc}$ and PrP 27−30 have hindered protein structure studies. Computational modeling of PrP provided an alternative approach by identifying those regions that are likely to adopt secondary structures (Cohen et al., 1994; Huang et al., 1994). These regions were then synthesized as peptides in sufficiently large quantities so that structural studies could be initiated (Gasset et al., 1992). While small PrP peptides are clearly imperfect models of PrP structure as demonstrated by the different secondary structures assumed by 104H1 and

H1 (Figure 1), some insight into the conformational transitions that feature in the formation of $PrP^{Sc}$ from $PrP^{C}$ (Pan et al., 1993) may be forthcoming from the use of synthetic PrP peptides.

While this work was in progress, it was reported that protease resistance can be induced in radiolabeled SHa $PrP^{C}$ by mixing with a large excess (>50-fold) of SHa $PrP^{Sc}$ (Kocisko et al., 1994). Both $PrP^{C}$ and $PrP^{Sc}$ were "partially" denatured in 3 M GdnHCl prior to mixing and then renatured as evidenced by protease resistance upon dilution of the GdnHCl. Whether Mo $PrP^{C}$ could be converted into $PrP^{Sc}$ with SHa $PrP^{Sc}$ under the conditions of these experiments was not reported. In studies of scrapie infectivity, renaturation from Gdn solutions could not be demonstrated as measured by bioassays of scrapie infectivity (Prusiner et al., 1993b). Furthermore, mixtures of equimolar amounts of $PrP^{C}$ and $PrP^{Sc}$ did not result in the measurable conversion of $PrP^{C}$ into $PrP^{Sc}$ (Raeber et al., 1992). Of note are the studies reported here where as little as 1% H1 initiated the conformational conversion of 104H1 (Figure 2). Whether the large excess of $PrP^{Sc}$ may have nonspecifically protected radiolabeled $PrP^{C}$ from proteolytic degradation with prior conversion of its conformation in the experiments of Kocisko et al. remains to be determined (Kocisko et al., 1994). Certainly, spectroscopic information about the physical state of PrP and bioassays of scrapie infectivity are required before firm conclusions can be drawn.

Although we have not fully eliminated the possibility that a covalent modification, which is difficult to detect, might trigger the conformational transition in $PrP^{C}$ that occurs *in vivo*, it is of interest that similar transitions can occur in PrP peptides *in vitro*. It is doubtful that a chemical modification triggers the conformational changes observed for PrP peptides. As described under Results, we have no evidence that PrP peptides undergo significant oxidation, which is thought to feature in the polymerization of the A$\beta$ peptide.

The sequence specificity of the conformational changes induced in PrP peptides is of considerable interest. In studies of H1 interacting with 104H1, a change of two residues in H1 corresponding to the Mo PrP sequence greatly lowers the efficacy of 104H1 conversion (Figure 3). In contrast, H1 also interacts with H2, but the sequence of H2 differs completely from that of H1. However, this interaction is also specific since A$\beta$ peptides do not convert H2. It is noteworthy that H1 consisting of PrP residues 109−122 is largely contained within the segment 113−128, which is conserved in all species studied to date, including PrP from chicken (Harris et al., 1991). Chicken PrP is otherwise only ~30% homologous with mammalian PrP (Gabriel et al., 1992).

The polymerization of PrP peptides into amyloid fibrils has been cited as evidence (Jarrett & Lansbury, 1993) in support of a crystallization mechanism proposed for prion replication (Gajdusek, 1988). Crystallization implies multidimensional macroscopic ordered arrays with a high degree of at least two-dimensional, and more commonly three-dimensional, organization of $PrP^{Sc}$. Despite the attractiveness of the amyloid model (Gajdusek, 1988, 1990; Gajdusek & Gibbs, 1990; Jarrett & Lansbury, 1993), there is no compelling evidence favoring formation of paracrystalline arrays of PrP amyloid as a mechanism for $PrP^{Sc}$ synthesis; to the contrary, an enlarging body of data militates against PrP amyloid formation in the propagation of prions (Prusiner, 1991). While the high $\beta$-sheet content of $PrP^{Sc}$ is clearly a hallmark distinguishing it from $PrP^{C}$ (Pan et al., 1993; Safar et al., 1993a), there is no evidence that $PrP^{Sc}$ forms paracrystalline arrays as is the case for amyloids, which also have a high $\beta$-sheet content (Glenner, 1980; Glenner et al., 1974). Purified infectious prions isolated from scrapie-infected SHa brains with a cocktail of protease inhibitors contain only $PrP^{Sc}$ which exists as amorphous aggregates; only if $PrP^{Sc}$ molecules are exposed to detergents and limited proteolysis, yielding PrP 27−30, do they then polymerize into prion rods exhibiting the ultrastructural and tinctorial features of amyloid (McKinley et al., 1991; Pan et al., 1993; Prusiner et al., 1983). Furthermore, dispersion of prion rods into detergent−lipid−protein complexes results in a 10−100-fold increase in scrapie titer, and no rods could be identified in these fractions by electron microscopy (Gabizon et al., 1987). The radiation target size of prions in liposomes and rods was measured as 55 ± 9 kDa, supporting the proposal that $PrP^{Sc}$ may be dimers (Bellinger-Kawahara et al., 1988). Consistent with these findings is the absence or rarity of amyloid plaques in many prion diseases as well as the inability to identify any amyloid-like polymers in cultured cells chronically synthesizing prions (McKinley et al., 1991; Prusiner et al., 1990). The concentration dependence of aggregation may further modify the details of the conformational interconversion of $PrP^{C}$ to $PrP^{Sc}$. At low concentration, the enthalpic advantage of aggregation may be offset by entropic factors.

While the energy barriers to these conformational isomerizations may be relatively modest in isolated peptides, it is possible that the equivalent processes for intact proteins *in vivo* require the intervention of molecular chaperones or other cellular factors. The specificity of prion replication has been demonstrated in studies of Tg mice where the prions produced were homologous to those in the inoculum; these findings argue for the formation of a $PrP^{C}/PrP^{Sc}$ complex during prion propagation (Prusiner et al., 1990). Of note, Tg(HuPrP) mice rarely produce $HuPrP^{Sc}$ after inoculation with Hu prions while Tg(MHu2M) mice expressing a chimeric $Hu/MoPrP^{C}$ readily produce chimeric $PrP^{Sc}$ after inoculation with Hu prions. These results suggest that a species-specific factor(s), possibly a chaperone-like molecule, bind(s) to the $PrP^{C}/PrP^{Sc}$ complex during the conversion process (Telling et al., 1994). Whether $PrP^{C}$ and $PrP^{Sc}$ are monomers or they exist as oligomers is unknown, but there is no evidence for large multimers which are implicit in the amyloid crystallization model (Prusiner, 1991).

This study provides some insight into the process whereby the "message" from $PrP^{Sc}$ might be transmitted to nascent $PrP^{C}$ through an interaction that affects a dramatic conformation change, without contravening accepted biological principles. Although H1 and other synthetic peptides have failed, to date, to induce prions in Syrian hamsters after intracerebral inoculation, additional studies seem warranted. The correlation of biological activity with the structure of PrP peptides would represent an important advance and allow determination of the conformational features of PrP that are required for $PrP^{Sc}$ formation.

## ACKNOWLEDGMENT

We thank Sherman Jew and Tatiana Livshits for synthesizing and purifying the peptides and acknowledge the

contributions of Maria Gasset, Darlene Groth, and Marilyn Torchia.

## REFERENCES


Ashburn, T. T., Auger, M., & Lansbury, P. T., Jr. (1992) *J. Am. Chem. Soc. 114*, 790−791.

Bellinger-Kawahara, C. G., Kempner, E., Groth, D. F., Gabizon, R., & Prusiner, S. B. (1988) *Virology 164*, 537−541.

Borchelt, D. R., Scott, M., Taraboulos, A., Stahl, N., & Prusiner, S. B. (1990) *J. Cell Biol. 110*, 743−752.

Borchelt, D. R., Taraboulos, A., & Prusiner, S. B. (1992) *J. Biol. Chem. 267*, 16188−16199.

Büeler, H., Fischer, M., Lang, Y., Bluethmann, H., Lipp, H.-P., DeArmond, S. J., Prusiner, S. B., Aguet, M., & Weissmann, C. (1992) *Nature 356*, 577−582.

Büeler, H., Aguzzi, A., Sailer, A., Greiner, R.-A., Autenried, P., Aguet, M., & Weissmann, C. (1993) *Cell 73*, 1339−1347.

Byler, D. M., & Susi, H. (1986) *Biopolymers 25*, 469−487.

Caughey, B., & Raymond, G. J. (1991) *J. Biol. Chem. 266*, 18217−18223.

Caughey, B. W., Dong, A., Bhat, K. S., Ernst, D., Hayes, S. F., & Caughey, W. S. (1991) *Biochemistry 30*, 7672−7680.

Cohen, F. E., Pan, K.-M., Huang, Z., Baldwin, M., Fletterick, R. J., & Prusiner, S. B. (1994) *Science 264*, 530−531.

Come, J. H., Fraser, P. E., & Lansbury, P. T., Jr. (1993) *Proc. Natl. Acad. Sci. U.S.A. 90*, 5959−5963.

Dyson, H. J., Rance, M., Houghten, R. A., Wright, P. E., & Lerner, R. A. (1988) *J. Mol. Biol. 201*, 201−217.

Forloni, G., Angeretti, N., Chiesa, R., Monzani, E., Salmona, M., Bugiani, O., & Tagliavini, F. (1993) *Nature 362*, 543−546.

Gabizon, R., McKinley, M. P., & Prusiner, S. B. (1987) *Proc. Natl. Acad. Sci. U.S.A. 84*, 4017−4021.

Gabriel, J.-M., Oesch, B., Kretzschmar, H., Scott, M., & Prusiner, S. B. (1992) *Proc. Natl. Acad. Sci. U.S.A. 89*, 9097−9101.

Gajdusek, D. C. (1988) *J. Neuroimmunol. 20*, 95−110.

Gajdusek, D. C. (1990) in *Virology* (Fields, B. N., Knipe, D. M., Chanock, R. M., Hirsch, M. S., Melnick, J. L., Monath, T. P., & Roizman, B., Eds.) 2nd ed., pp 2289−2324, Raven Press, New York.

Gajdusek, D. C., & Gibbs, C. J., Jr. (1990) in *Biomedical Advances in Aging* (Goldstein, A., Ed.) pp 3−24, Plenum Press, New York.

Gasset, M., Baldwin, M. A., Lloyd, D., Gabriel, J.-M., Holtzman, D. M., Cohen, F., Fletterick, R., & Prusiner, S. B. (1992) *Proc. Natl. Acad. Sci. U.S.A. 89*, 10940−10944.

Gasset, M., Baldwin, M. A., Fletterick, R. J., & Prusiner, S. B. (1993) *Proc. Natl. Acad. Sci. U.S.A. 90*, 1−5.

Glenner, G. G. (1980) *N. Engl. J. Med. 302*, 1283−1292.

Glenner, G. G., Eanes, E. D., Bladen, H. A., Linke, R. P., & Termine, J. D. (1974) *J. Histochem. Cytochem. 22*, 1141−1158.

Goldfarb, L. G., Petersen, R. B., Tabaton, M., Brown, P., LeBlanc, A. C., Montagna, P., Cortelli, P., Julien, J., Vital, C., Pendelbury, W. W., Haltia, M., Wills, P. R., Hauw, J. J., McKeever, P. E., Monari, L., Schrank, B., Swergold, G. D., Autilio-Gambetti, L., Gajdusek, D. C., Lugaresi, E., & Gambetti, P. (1992) *Science 258*, 806−808.

Halverson, K. J., Sucholeiki, I., Ashburn, T. T., & Lansbury, P. T., Jr. (1991) *J. Am. Chem. Soc. 113*, 6701−6703.

Harris, D. A., Falls, D. L., Johnson, F. A., & Fischbach, G. D. (1991) *Proc. Natl. Acad. Sci. U.S.A. 88*, 7664−7668.

Hensley, K., Carney, J. M., Mattson, M. P., Aksenova, M., Harris, M., Wu, J. F., Floyd, R. A., & Butterfield, D. A. (1994) *Proc. Natl. Acad. Sci. U.S.A. 91*, 3270−3274.

Huang, Z., Gabriel, J.-M., Baldwin, M. A., Fletterick, R. J., Prusiner, S. B., & Cohen, F. E. (1994) *Proc. Natl. Acad. Sci. U.S.A. 91*, 7139−7143.

Jarrett, J. T., & Lansbury, P. T., Jr. (1993) *Cell 73*, 1055−1058.

Johnson, W. C., Jr. (1990) *Proteins: Struct., Funct., Genet. 7*, 205−214.

Kocisko, D. A., Come, J. H., Priola, S. A., Chesebro, B., Raymond, G. J., Lansbury, P. T., Jr., & Caughey, B. (1994) *Nature 370*, 471−474.

Krimm, S., & Bandekar, J. (1986) *Adv. Protein Chem. 38*, 181−364.

McKinley, M. P., Meyer, R., Kenaga, L., Rahbar, F., Cotter, R., Serban, A., & Prusiner, S. B. (1991) *J. Virol. 65*, 1440−1449.

Otvos, L., Jr., Szendrei, G. I., Lee, V. M., & Mantsch, H. H. (1993) *Eur. J. Biochem. 211*, 249−257.

Pan, K.-M., Baldwin, M., Nguyen, J., Gasset, M., Serban, A., Groth, D., Mehlhorn, I., Huang, Z., Fletterick, R. J., Cohen, F. E., & Prusiner, S. B. (1993) *Proc. Natl. Acad. Sci. U.S.A. 90*, 10962−10966.

Pattison, I. H. (1965) in *Slow, Latent and Temperate Virus Infections, NINDB Monograph 2* (Gajdusek, D. C., Gibbs, C. J., Jr., & Alpers, M. P., Eds.) pp 249−257, U. S. Government Printing, Washington, D.C.

Pike, C. J., Burdick, D., Walencewicz, A. J., Glabe, C. G., & Cotman, C. W. (1993) *J. Neurosci. 13*, 1676−1687.

Prusiner, S. B. (1991) *Science 252*, 1515−1522.

Prusiner, S. B., McKinley, M. P., Bowman, K. A., Bolton, D. C., Bendheim, P. E., Groth, D. F., & Glenner, G. G. (1983) *Cell 35*, 349−358.

Prusiner, S. B., Scott, M., Foster, D., Pan, K.-M., Groth, D., Mirenda, C., Torchia, M., Yang, S.-L., Serban, D., Carlson, G. A., Hoppe, P. C., Westaway, D., & DeArmond, S. J. (1990) *Cell 63*, 673−686.

Prusiner, S. B., Groth, D., Serban, A., Koehler, R., Foster, D., Torchia, M., Burton, D., Yang, S.-L., & DeArmond, S. J. (1993a) *Proc. Natl. Acad. Sci. U.S.A. 90*, 10608−10612.

Prusiner, S. B., Groth, D., Serban, A., Stahl, N., & Gabizon, R. (1993b) *Proc. Natl. Acad. Sci. U.S.A. 90*, 2793−2797.

Raeber, A. J., Borchelt, D. R., Scott, M., & Prusiner, S. B. (1992) *J. Virol. 66*, 6155−6163.

Safar, J., Roller, P. P., Gajdusek, D. C., & Gibbs, C. J., Jr. (1993a) *J. Biol. Chem. 268*, 20276−20284.

Safar, J., Roller, P. P., Gajdusek, D. C., & Gibbs, C. J. J. (1993b) *Protein Sci. 2*, 2206−2216.

Schätzl, H. M., Da Costa, M., Taylor, L., Cohen, F. E., & Prusiner, S. B. (1995) *J. Mol. Biol. 245*, 362−374.

Scott, M., Groth, D., Foster, D., Torchia, M., Yang, S.-L., DeArmond, S. J., & Prusiner, S. B. (1993) *Cell 73*, 979−988.

Selvaggini, C., De Gioia, L., Cantu, L., Ghibaudi, E., Diomede, L., Passerini, F., Forloni, G., Bugiani, O., Tagliavini, F., & Salmona, M. (1993) *Biochem. Biophys. Res. Commun. 194*, 1380−1386.

Stahl, N., Baldwin, M. A., Hecker, R., Pan, K.-M., Burlingame, A. L., & Prusiner, S. B. (1992) *Biochemistry 31*, 5043−5053.

Stahl, N., Baldwin, M. A., Teplow, D. B., Hood, L., Gibson, B. W., Burlingame, A. L., & Prusiner, S. B. (1993) *Biochemistry 32*, 1991−2002.

Surewicz, W. K., & Mantsch, H. H. (1988) *Biochim. Biophys. Acta 952*, 115−130.

Taylor, J. W., & Kaiser, E. T. (1987) *Methode Enzymol. 154*, 473−498.

Telling, G. C., Scott, M., Hsiao, K. K., Foster, D., Yang, S.-L., Torchia, M., Sidle, K. C. L., Collinge, J., DeArmond, S. J., & Prusiner, S. B. (1994) *Proc. Natl. Acad. Sci. U.S.A. 91*, 9936−9940.

Wu, L. C., Laub, P. B., Elöve, G. A., Carey, J., & Roder, H. (1993) *Biochemistry 32*, 10271−10276.


BI9424959